

# Impact of operating conditions on the evolution of droplet penetration in oil mist filters

T. Penner\*, J. Meyer, G. Kasper, A. Dittler

*Institut für Mechanische Verfahrenstechnik und Mechanik, Karlsruhe Institute of Technology, Germany*

## ABSTRACT

The operating conditions of oil mist filters along with the filter media properties are the decisive factors for the evolution of separation efficiency and pressure drop during filter operation. Experimental studies were carried out to determine the evolution of clean gas concentration of oil mist filters with different media properties with regard to the oil transport mechanisms and its dependence on the operating conditions of the filters. The experiments were carried out using two types of glass fiber filter media, one oleophilic and one oleophobic. The effects of filter face velocity and oil loading rate were investigated for both filter media. The effect of media thickness was explored by varying the number of layers. It was found that filter overall separation efficiency can be correlated with the oil transport mechanisms analogously to the correlation to pressure drop proposed by the Film-and-Channel model by Kampa et al. (2004). Decreasing velocities led to a stronger increase in overall penetration when liquid channels are formed in both types of media, which can be attributed to a loss of efficiency for droplets smaller than the MPPS in the size range of 0.1  $\mu\text{m}$  and below, while increasing the oil loading rate had the same effect, however not as distinct. Increasing filter thickness by adding filter layers also caused a stronger increase of penetration during this channel section. The formation of an oil film caused a drop in penetration. The effect of the oil film on penetration was found to be independent of loading rate, but not of velocity, due to its significance for inertial deposition. For highly efficient oleophilic filters, entrainment was found to be the dominant factor for clean gas concentration in steady state.

## 1. Introduction

Oil mist in the submicron size range, i.e. aerosol consisting of oil droplets smaller than 1  $\mu\text{m}$ , is emitted by oil lubricated gas compressors, metal cutting and engine crankcase ventilation, amongst other industrial processes. As this mist poses a risk to human health and the environment [2,3] it needs to be removed from gas streams. Coalescence filters are commonly used to separate oil droplets from air streams and glass fiber filter media are used for applications where high efficiencies are required, for instance for compressed air preparation. Commercially available oil mist filters mostly consist of several layers of oleophilic or oleophobic (i.e. wettable or non wettable with oil) glass fiber media. From previous investigations it is well known that the operating characteristics of such filters change significantly over time, which is caused by the loading of the filters with oil and the transport of deposited oil inside the filter media. Kampa et al. [1] describe the mechanisms of oil transport through filter media and the contribution of the local oil distribution inside the filter media to the overall differential pressure  $\Delta p$  of the filter in the Film and Channel model. The overall differential pressure of an oil mist filter according to this model consists of the  $\Delta p_{dry}$  of the dry filter, a  $\Delta p_{channel}$  caused by filter areas blocked by coalesced droplets, which are transported through the media in multiple parallel channel like structures resulting in a

decreased effective porosity of the media and a  $\Delta p_{jump}$  caused by the formation of a thin liquid film on the filter face. Whether the film forms on the filter front or back face and thus occurs at the beginning of filter operation or before reaching a steady state, depends on the wettability of the filter media.

The influence of operating conditions on the pressure drop and internal oil saturation of a filter was investigated by Kolb et al. [4]. It was found that any increase in velocity leads to a decrease of saturation in steady state, while excess  $\Delta p$ , which is the sum of  $\Delta p_{jump}$  and  $\Delta p_{channel}$  remained independent of filtration velocity. Saturation and  $\Delta p_{channel}$  increased with loading rate, while  $\Delta p_{jump}$  was not affected. Filter efficiency was not considered. Several studies investigating the evolution of filter efficiency when loading with liquid aerosols conclude that overall efficiency decreases during filter operation [5-8] and that the decrease in efficiency depends on operating conditions and physico-chemical characteristics of the aerosol filtered, specifically the surface tension of the liquids, and that changes in efficiency correspond to changes in pressure drop [7,9]. According to these findings, the liquid transport mechanisms in the filter media have an immediate effect on filter efficiency, however, the changes in filter efficiency weren't linked to the transport mechanisms according to the Film and Channel Model. Kampa et al. have shown that rather than surface tension of the droplets, the wettability of the media with the deposited liquid is decisive.

\* Corresponding author.

E-mail address: thomas.penner@kit.edu (T. Penner).

The wettability of the filter not only affects the evolution of pressure drop and efficiency, but was also found to be crucial for entrainment, as was shown by Wurster et al. [10,11]. Entrainment of droplets mainly occurs at steady state with the main mechanism being bursting bubbles rather than blown off droplets on the filter downstream face, independent of media wettability. Other studies on the contrary conclude that efficiency increases during operation. Conder and Liew [12] found that efficiency is increased by wet operation with the exception of low filtration velocities, which they attribute to an increased single fiber efficiency due to decreased effective porosity and associated distortion of flow field. Charvet et al. [13] observed that filter efficiency improves during filter operation, especially for bigger droplets, and it increases with filtration velocity. In another study Charvet et al. [14] found that during filter operation efficiency decreases for droplets smaller than the most penetrating particle size (MPPS), while it increases for bigger droplets and conclude that this effect results from the increase of local velocities inside the filter media due to the accumulation of liquid in the filter. They do however not take into account the effects of liquid transport mechanisms and different wettabilities of the filter media.

The aim of this work is to study the evolution of filter separation efficiency and pressure drop and thus linking effects of liquid transport mechanisms to filter overall separation efficiency. In this context the influence of operating conditions and media properties, specifically the wettability with oil, on penetration during loading and steady state is investigated. Experiments were performed with different filtration velocities, loading rates, two types of glass fiber filter media and various filter thicknesses, i.e. number of filter layers, with oil mist generated from a commercially used compressor oil. Differential pressure, penetration, both total and size resolved, and filter saturation were measured.

## 2. Experimental setup and methods

All experiments described in this paper were carried out by loading an initially dry stack of filter layers with oil mist under well controlled parameters for each run, listed in Table 1. Each run was continued until steady state was reached. Steady state was assumed when drainage flow from the back face of the filter was detected, i.e. when the first drop of oil was captured in the balance, about 10–30 min (depending on operating conditions) after a horizontal pressure drop curve was attained and several minutes after drainage occurs at the back of the filter, as liquid transport to the balance takes some time. Oil mist generation and air flow was then shut off to examine the filter layers. Total duration of each run was 1–10 h, depending on operating conditions.

Oil mist was generated by one or two Collison type nebulizers from a commercially used compressor lubricant oil (dynamic viscosity 0.122 Pa·s, surface tension of 0.031 N/m, density 0.9 g/cm<sup>3</sup>, properties at standard conditions). The droplet size of the generated aerosol was roughly log normal distributed with a number based mean around 350 nm and a standard deviation of 1.8 as repeatedly measured with a Scanning Mobility Particle Sizer (SMPS) at ambient temperatures in the range of 19.5–21.5 °C and pressure in the range between 1.009 and 1.015 bar. Generated oil mist rate was kept constant for each run by maintaining a constant differential pressure across the nebulizer during

**Table 1**  
Parameters varied in the experiments.

Varied parameters	values
filtration velocity	10 cm/s
	25 cm/s
	40 cm/s
oil loading rate	60 mg/(m <sup>2</sup> s)
	90 mg/(m <sup>2</sup> s)
	195 mg/(m <sup>2</sup> s)
number of layers	4, 6, 8 and 10 layers

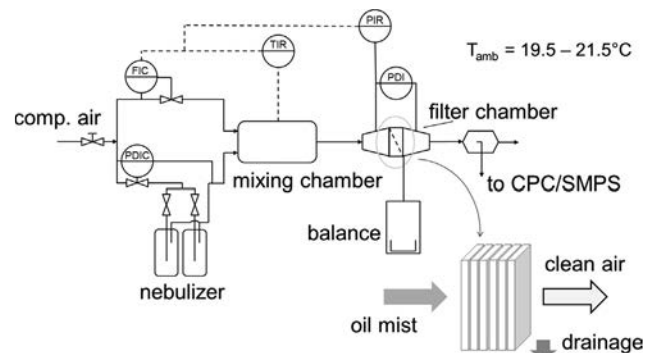


**Fig. 1.** Schematic diagram of the experimental set-up consisting of one (or two) nebulizer(s), a temperature and absolute pressure corrected make-up flow by a mass flow controller, which is mixed with the aerosol in a mixing chamber and a filter chamber, where drained oil is collected and recorded gravimetrically. Clean gas concentration is monitored constantly.

filter operation. The oil mist was mixed with dry air in a mixing chamber to adjust the desired filter face velocity. Absolute pressure and temperature were constantly monitored on the raw gas side of the filter and the effect of increasing pressure and changing temperature on flow rate were compensated by adjusting the mass flow to maintain a constant filter face velocity. A schematic diagram of the experimental set up is given in Fig. 1.

The used filter specimens were stacks of flat nonwoven glass fiber filter media commonly used for industrial applications with an effective filtration area of 8 cm × 8 cm and a metal grid support at the back face of the filter. Two media were used, one oleophilic and one oleophobic medium, that differed not only in their wettabilities, but also in structural properties. Even though differences in differential pressure and filter efficiency can also be attributed to these structural differences, the relative changes in their operating characteristics are typical for oleophilic and oleophobic media respectively. Characteristic media properties are listed below in Table 2.

During operation pressure drop was monitored and recorded continuously. Oil draining from the back of the filter was measured by a balance recording the accumulated oil mass. As entrainment rates were negligible compared to loading rates and overall filter separation efficiencies were > 99%, filter loading rates were determined from drainage rates. Clean gas concentration was continuously monitored and recorded during operation with a Condensation Particle Counter (CPC). In the evaluation of the measurements, penetration was normalized by calculating the penetration to dry penetration ratio, choosing the clean gas concentration of the respective medium and number of layers in dry state as a reference. SMPS samples were taken at distinct points in time. To determine possible influence of entrainment on clean gas concentration in steady state, the nebulizer was shut off while air flow remained constant and clean gas concentration was monitored for another 5 min before air flow was shut off and the filter element was taken out. Before and after each run layers were separated and weighted to determine liquid saturation of each layer as well as the global saturation of the filter. To eliminate errors induced by the clamping of the filter, the edges of the layers, where they were clamped in the metal frame, were removed after each run before weighting the layers. As the liquid film forming on the downstream side of oleophilic filters

**Table 2**  
Properties of the filter media layers used in the experiments.

Medium	wettability	Porosity [-]	Single layer thickness [mm]	Mean pore size [μm]
A	oleophilic	0.94	0.5	7
B	oleophobic	0.95	0.8	11

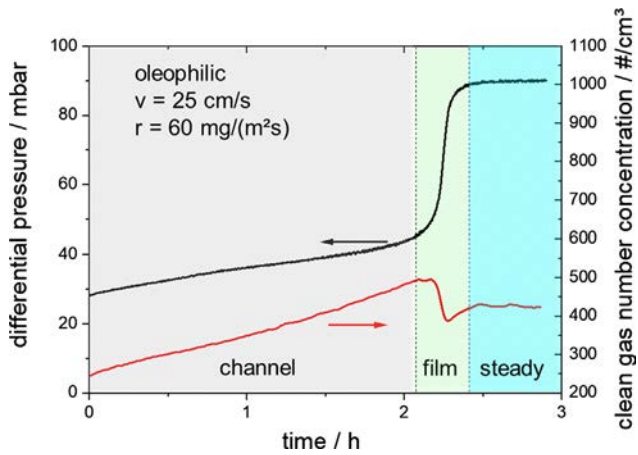


Fig. 2. Evolution of pressure drop and clean gas concentration for an oleophilic filter medium.

collapses when shutting off the air flow, and thus causes the last layer to contain additional oil, the last layer of filter medium was excluded from this measurement.

### 3. Results and discussion

#### 3.1. Evolution of pressure drop and clean gas concentration in oleophilic and oleophobic media

Analogous to the effects observed in the evolution of differential pressure during filter operation, the different stages of filter loading and mechanisms of oil transport through the media bear a considerable effect on the evolution of filter penetration, which becomes obvious in the changes of clean gas concentration occurring simultaneously to changes in pressure drop. While the Film and Channel model describes the relationship between pressure drop and liquid transport mechanisms in filter media, the conclusions about the transport mechanisms can also be applied to the effects on filter penetration, as seen in Fig. 2.

For oleophilic filters in the first stage of operation differential pressure rises linearly as deposited droplets coalesce and form channels, which subsequently transport deposited oil through the filter medium. This channel stage of operation is characterized by an increase in differential pressure  $\Delta p_{channel}$ . Parallel to the increasing differential pressure a steady, linear rise in clean gas concentration is observed in this stage. This is due to the loss of collector surface and changes in fiber geometry caused by deposited and coalesced droplets. Additionally, gas velocity inside the filter is increased due to decreased effective porosity of the filter causing a decrease of diffusional deposition and thus a deterioration of efficiency for smaller droplets. For the velocities and loading rates used in this study, the calculated increase of mean internal velocity amounted to 15–40 percent compared to internal velocity of the dry filters. In the second stage of operation differential pressure increases rapidly. In this film stage the channels formed in the first stage reach the back face of the filter and the oil forms a film, which causes a steep jump in differential pressure  $\Delta p_{jump}$ . The formation of the film is associated with a drop in clean gas concentration. Gas passing the filter is diverted through holes in the film. The diversion of the aerosol causes inertial impaction of droplets on the film, thus increasing the efficiency of the filter, so the liquid film can be seen as sort of a perforated plate in terms of aerosol deposition. Before steady state is reached clean gas concentration increases slightly before stabilizing when reaching steady state, while differential pressure remains almost constant. After disconnecting the nebulizer while maintaining air flow, aerosol is still present in the scale of the small rise of concentration before steady state, so it can be assumed that this rise in penetration is not caused by primary penetration but rather by entrainment of

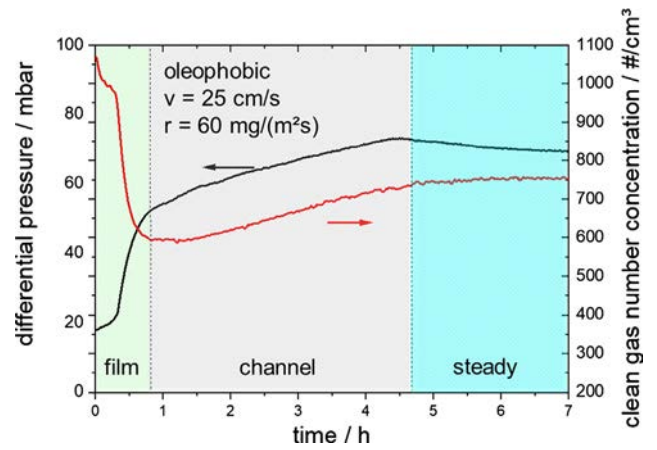


Fig. 3. Evolution of pressure drop and clean gas concentration for an oleophobic filter medium.

droplets at the back of the filter. This conclusion is further supported as the bursting of bubbles is observed at the back face of the filter, which has been shown to be the primary mechanism of entrainment for oleophilic filter media by Wurster et al. [10].

Oleophobic filter media behave in the opposite way regarding the sequence of oil transport mechanisms, as deposited oil form the liquid film in the first stage of filter operation on the front face of the filter. As a result,  $\Delta p_{jump}$  and the drop in clean gas number concentration occur at the beginning of filter operation (see Fig. 3). When the differential pressure is high enough, oil is pushed into subsequent layers, where it forms channels. As in the channel stage of oleophilic filters, this leads to a linear rise in of differential pressure  $\Delta p_{channel}$  and clean gas concentration. Differential pressure and clean gas concentration reach steady state as the channels reach the back of the filter, forming growing droplets until these droplets drain due to gravity. No significant entrainment can be observed for the oleophobic filter medium.

As the film has a bigger impact on clean gas concentration for oleophobic filters it might be concluded, that it has a higher separation efficiency. However, it has to be taken into account that the aerosol arriving at the film of oleophilic filters is expected to have a different particle size distribution and concentration compared to the aerosol arriving at the film of oleophobic filters, as the aerosol is filtrated in preceding layers before reaching the film on the downstream side of the filter. Furthermore it has to be considered that the gas flow conditions on the upstream side of the filter differ greatly from the conditions inside the filter media adding to a different depositional behavior of the aerosol. The differences in the absolute values of pressure drop and overall penetration between the two types of filters are not only to be attributed to the different wettabilities of the two materials, but also to the differences in their structural properties.

#### 3.2. Impact of filtration velocity and loading rate on droplet penetration

Previous investigations have shown that the saturation of filters in steady state depends on operational parameters, such as filtration velocity and loading rate [4]. As liquid saturation of filter media directly affects effective porosity and the collector surface of the filter exposed to the aerosol flow, it is expected to have an effect also on evolution of filter efficiency when loading with oil. To proof the influence of operating parameters on filter overall efficiency filters consisting of six layers of oleophilic and oleophobic filter media, respectively, were loaded with oil mist at a constant rate of  $60 \text{ mg}/(\text{m}^2\text{s})$  and filter face velocities of 10, 25 and  $40 \text{ cm}/\text{s}$ , which equals oil mist concentrations of  $600 \text{ mg}/\text{m}^3$ ,  $240 \text{ mg}/\text{m}^3$  and  $150 \text{ mg}/\text{m}^3$ , respectively.

Fig. 4 shows the evolution of penetration to dry penetration ratio and excess  $\Delta p$  over cumulative oil mass for oleophilic and oleophobic

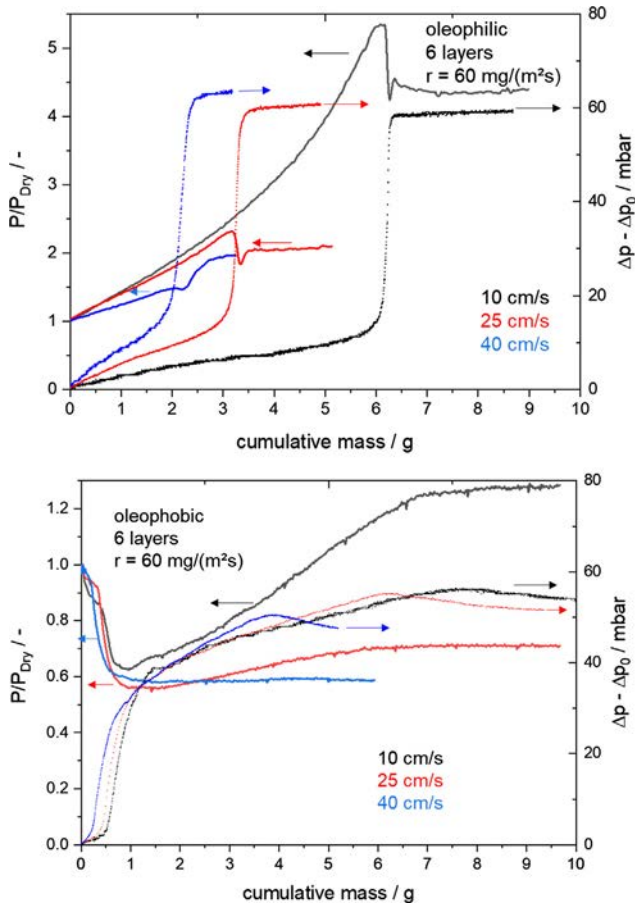


Fig. 4. Penetration to dry penetration ratio and excess  $\Delta p$  over cumulative oil mass for different velocities for oleophilic and oleophobic filters.

filters and velocities of 10, 25 and 40 cm/s. For both types of media, steady state is reached for lower cumulative oil masses at higher velocities. For oleophilic filters the jump in differential pressure and drop in overall penetration, which indicate the formation of the film, occurs at lower oil masses, thus resulting in a shorter increase of differential pressure and overall penetration in the channel stage. The channel  $\Delta p$  section becomes steeper with increasing velocities, resulting in a  $\Delta p_{channel}$ , which is independent of filtration velocity. The slopes of the curves for overall penetration in this section are roughly the same, meaning the deterioration of overall efficiency decreases with increasing velocities. When a film is formed on the downstream side of the filter penetration decreases rapidly. For 40 cm/s however, the penetration to dry penetration ratio shows a more pronounced increase immediately before reaching steady state, when compared to lower velocities. This is not due to primary penetration, but an increased proportion of entrainment in clean gas concentration. Excess  $\Delta p$  of the oleophilic filters does not change significantly with velocity, reaching a value of about 60 mbar.

For the oleophobic filters the drop in penetration to dry penetration ratio increases between 10 and 25 cm/s, seen in Fig. 4 emphasizing the significance of the film for inertial impaction. As the increase of penetration in the channel section decreased with velocity, higher velocities resulted in an improved overall filter efficiency. For 40 cm/s, no significant increase of penetration after the formation of the film can be seen. The  $\Delta p_{jump}$  apparently decreased with velocity, while  $\Delta p_{channel}$  was independent of velocity, as for the oleophilic filters. The differences of the  $\Delta p_{jump}$  cannot be explained with the Film and Channel Model and might be due to differences between different batches of the same medium.

The higher loss of overall efficiency that can be seen in the channel

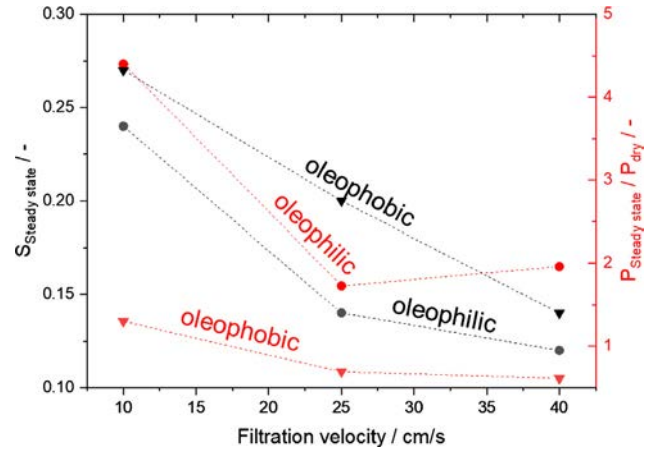


Fig. 5. Global steady state saturations and corresponding penetration ratios of oleophilic and oleophobic filters for different filtration velocities.

section for both types of media at lower velocities can be attributed to a higher loss of collector surface through the clogging of fiber sections due to higher liquid saturations at lower velocities. This can be seen in Fig. 5, which shows global steady state saturations and steady state to dry state penetration ratios of both types of filter media over filtration velocity. It shows that along with a decreasing steady state saturation, which is due to the higher differential pressure at higher velocities, which acts on the saturation of a filter in a manner, similar to an increasing pressure gradient over a system of capillaries filled with liquid, the steady state to dry state penetration ratio decreases with increasing velocity for both types of media, with the exception of  $P_{Steady\ state}/P_{dry}$  for 40 cm/s of the oleophilic medium, which is due to entrainment, as explained above. It also shows the improvement of overall efficiency for the oleophobic medium for 25 and 40 cm/s ( $P_{Steady\ state}/P_{dry} < 1$ ).

To determine the change of fractional efficiency of the filters due to loading at different filtration velocities, SMPS measurements on the downstream side of the filters were taken in dry and steady state for 10, 25 and 40 cm/s for the oleophobic medium only, as entrainment distorted the results for the oleophilic medium. Fig. 6 shows fractional efficiencies of the oleophobic filters at 10, 25 and 40 cm/s in dry and steady state. The efficiency at the MPPS in dry state decreases from over 99.5% for 10 cm/s to around 97% for 40 cm/s, as the MPPS decreases from 130 nm for 10 cm/s to 85 nm for 40 cm/s, due to the deterioration of diffusional deposition with increasing velocity. In steady state at

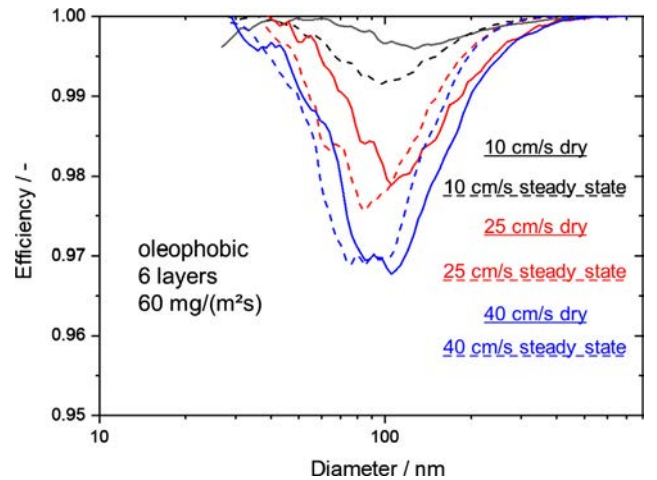


Fig. 6. Fractional grade efficiencies for 6 layers of a oleophobic filter medium in dry state and steady state for 10 cm/s, 25 cm/s and 40 cm/s filter face velocity at a loading rate of  $60\text{ mg}/(\text{m}^2\text{s})$ .

10 cm /s, it can be seen that efficiency is lost for all size fractions except for sizes above 200 nm, where efficiency actually improves, when compared to dry state efficiencies. The MPPS shifts to around 100 nm, while efficiency at the MPPS decreases to around 99%. For higher velocities, the efficiency in steady state increases for all sizes above the dry state MPPS, while it decreases for smaller sizes. This is due to the deterioration of diffusional deposition due to oil saturated areas inside the filter and presumably changed effective fiber geometries. The increase of efficiency for bigger droplets is due to the effect of the oil film, which acts as an inertial separator. The improvement of efficiency for bigger droplets increases with velocity, while deterioration for smaller droplets decreases, as saturations decrease (see Fig. 5).

To determine the effect of loading rate on penetration, six layers of oleophilic and oleophobic filter media were loaded with a constant filter face velocity of 25 cm/s and oil loading rates of 60 mg/(m<sup>2</sup>s) ( $\triangleq$  240 mg/m<sup>3</sup>), 90 mg/(m<sup>2</sup>s) ( $\triangleq$  360 mg/m<sup>3</sup>) and 195 mg/(m<sup>2</sup>s) ( $\triangleq$  780 mg/m<sup>3</sup>) respectively. According to the Film and Channel Model, oil loading rate is expected to have no impact on  $\Delta p_{jump}$ , it does however determine  $\Delta p_{channel}$  and liquid saturation in steady state. Therefore, oil loading rate should obviously have no impact on the formation of the film.

Fig. 7 shows penetration to dry penetration ratio and excess differential pressure over cumulative oil mass for oleophilic and oleophobic filters at oil loading rates of 60, 90 and 195 mg/(m<sup>2</sup>s). For both types of media, steady state is reached at slightly higher cumulative oil masses when increasing oil loading rate, as more oil needs to be transported through the media in a higher number oil channels [4]. For the oleophilic medium, initial penetration is roughly the same for all loading rates. With increasing cumulative oil mass, the curves for penetration to dry penetration ratio roughly increase with the same steady

slope for all three loading rates. As steady state is reached for only slightly higher cumulative oil masses at higher loading rates, penetration to dry penetration ratio in steady state does not differ significantly for all three loading rates. Excess differential pressure increases by roughly 10 mbar between loading rates of 60 mg/(m<sup>2</sup>s) and 195 mg/(m<sup>2</sup>s). This increase is only due to a higher  $\Delta p_{channel}$  caused by higher saturations, while  $\Delta p_{jump}$  is independent of loading rate.

For oleophobic filters at cumulative oil masses up to 0.5 g there is a slight difference in the three curves' progressions, presumably due to differences in the initial deposition of oil droplets and therefore changes in effective fiber geometries before enough oil is deposited to form a film. The curves coincide at cumulative oil masses greater than 0.5 g and are almost identical up to 1 g cumulative mass, which marks the end of the film formation, where penetration to dry penetration ratio drops to around 0.55 for all three loading rates. In the subsequent channel stage, the curves take an almost identical progression initially, however they reach steady state at different cumulative oil masses. Penetration to dry penetration ratio in steady state does not significantly change with loading rate. Similarly, the slopes of the curves for excess differential pressure are the same in the channel stage, differing only in the length of the channel stage leading to a different  $\Delta p_{channel}$  for each loading rate. The differences in excess differential pressure however, are not only due to a different  $\Delta p_{channel}$ , as  $\Delta p_{jump}$  increases with loading rate. This effect cannot be explained with the Film and Channel model and needs further investigation.

The differences in the lengths of the channel section and higher cumulative oil masses in steady state are also reflected in the measured global saturations. Fig. 8 shows global steady state saturations and steady state to dry state penetration ratios of both types of filter media over loading rate. Saturation increases slightly from 0.14 to 0.16 when increasing loading rate from 60 to 195 mg/(m<sup>2</sup>s) for the oleophilic medium and from 0.19 to 0.22 for the oleophobic medium. Considering differences between different batches of the same medium, which might possibly result in different values for steady state saturation, this slight increase is not necessarily only to be attributed to the increased loading rate. Steady state to dry state penetration ratio shows a minor increase from 2.11 to 2.18 for the oleophilic and from 0.68 to 0.7 for the oleophobic medium.

When comparing the performance of oleophilic and oleophobic filters in terms of change in penetration (see Fig. 9), it can be seen that the increase of penetration in the section where channels are formed is less distinguished for the oleophobic filters compared to the oleophilic filters, seen as a steeper slope of the penetration in Fig. 9, while the effect of the film on penetration is significantly higher for oleophobic filters, due to the differing aerosol concentration and droplet sizes

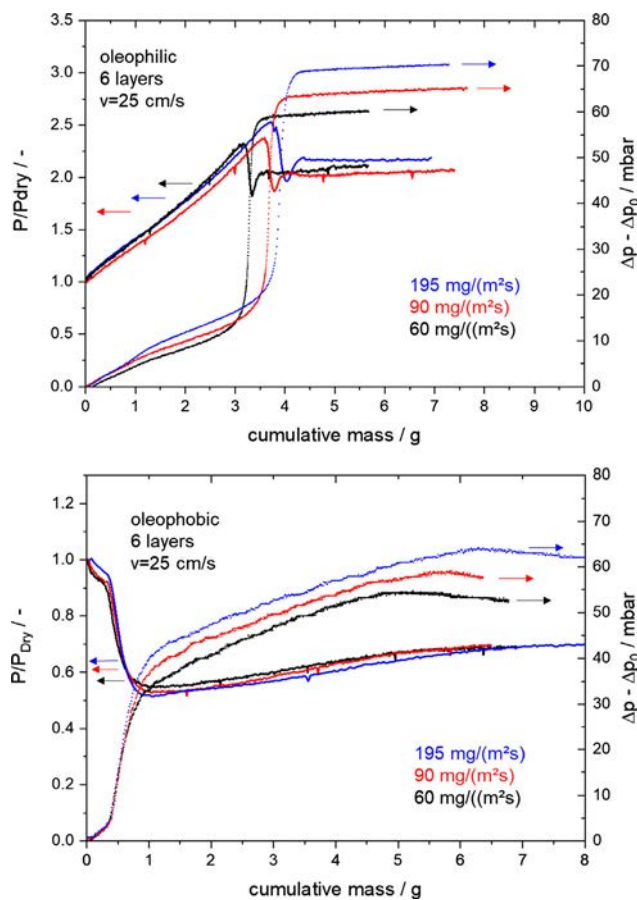


Fig. 7. Penetration to dry penetration ratio and excess  $\Delta p$  over cumulative mass for different loading rates for oleophilic and oleophobic filters.

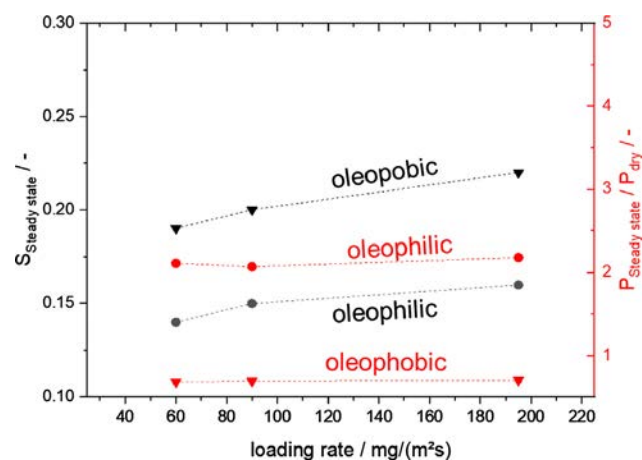


Fig. 8. Global steady state saturations and corresponding penetration to dry penetration ratios of oleophilic and oleophobic filters loaded with different oil loading rates.

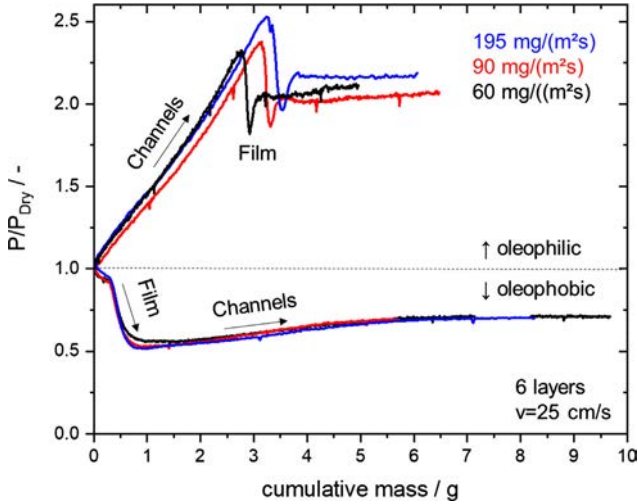


Fig. 9. Comparative performance of oleophilic and oleophobic filters regarding the penetration to dry penetration ratio loaded with different loading rates.

upstream of the film due to collection in the preceding channel section of oleophilic filters. No significant effect of loading rate on steady state penetration for the oleophobic filter medium can be seen, leading to an improved overall separation efficiency in steady state compared to the dry state for all loading rates. Overall separation efficiency in steady state is comparable for both types of filters even though it was considerably higher for the oleophilic filters in dry state. This effect might not necessarily be attributed to the wettability of the filters, as it also has to be considered that the two filter media used differ in their structural properties.

### 3.3. Impact of filter thickness

Apart from operating conditions, the effect of media thickness on the evolution of penetration during filter loading was investigated by adding layers to or removing layers of filter media from the filter. For each medium, 4, 6, 8 and 10 layers, respectively, were tested with a steady loading rate of  $60 \text{ mg}/(\text{m}^2\text{s})$  and a filter face velocity of  $25 \text{ cm}/\text{s}$ . According to the Film and Channel model, the jump in differential pressure caused by the film is independent from media thickness, while  $\Delta p_{\text{channel}}$  increases with media thickness. Hence, the formation of the film is not influenced, while the length of the channels increases with media thickness directly affecting  $\Delta p_{\text{channel}}$ .

Fig. 10 shows penetration to dry penetration ratio and excess differential pressure over cumulative oil mass for oleophilic and oleophobic filters with 4, 6, 8 and 10 filter layers initially. The progression of excess differential pressure and change in penetration to dry penetration ratio is almost identical for all filters. However, steady state is however reached at higher cumulative oil masses for an increasing number of layers, as the oil channels stretch across greater lengths before reaching the downstream side of the filter. Penetration in dry state decreases by almost one order of magnitude when adding two media layers for the oleophilic filters. The slopes of the curves in the channel stage are the same for all numbers of layers tested, as oil channels penetrate through the medium and subsequent formerly dry layers are saturated with oil. When these channels penetrate through a higher number of layers, steady state is reached at higher cumulative oil masses, leading to higher loss of total number efficiency in the channel stage relative to efficiency in dry state. Before reaching steady state penetration drops for four and six layers, however it increases rapidly for eight and ten layers, leading to a total penetration in steady state, which is up to one magnitude higher than total penetration of the dry filter in case of ten layers of the oleophilic medium. This is caused by bursting bubbles on the downstream side of the filter. As bubbles start

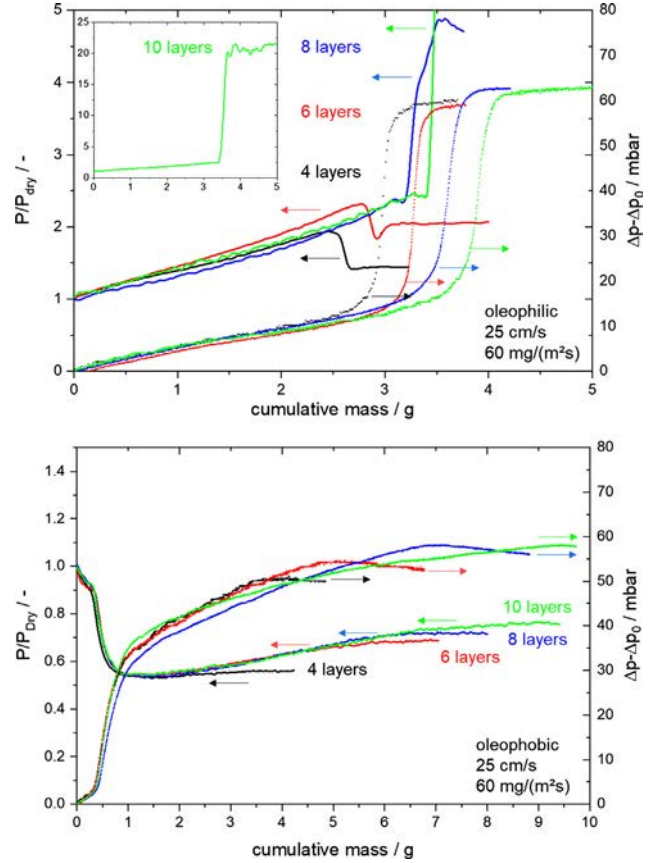


Fig. 10. Penetration to dry penetration ratio and excess  $\Delta p$  over cumulative oil mass for different number of filter layers for oleophilic and oleophobic filters.

bursting on the filter back face before the complete formation of the film, the entrained droplets cover up the effect of the film on total penetration, leading to a rapid increase of penetration. As the total number concentration of droplets produced by entrainment is independent of the number of layers, this effect is not seen for a lower number of layers, where primary penetration is considerably higher than secondary penetration by entrainment. Thus adding more layers than ten would not be practical, as clean gas droplet concentration in steady state would not be significantly reduced. The difference in total excess differential pressure is relatively low at 5 mbar between four and ten filter layers when compared to the differential pressure of the dry filters, where differential pressure the difference between four and ten layers is around 30 mbar. This difference is only due to an increased  $\Delta p_{\text{channel}}$ ,  $\Delta p_{\text{jump}}$  is independent of the number of layers.

For the oleophobic medium, the impact of the oil film on penetration to dry penetration ratio is independent of the number of layers, as penetration dropped by around 50% in all cases during the formation of the film on the filter front face. Similar the oleophilic medium the slopes of the curves in the channel stage are the same for all numbers of layers tested and steady state is reached at higher cumulative oil masses. No significant impact of entrainment on clean gas concentration is seen for any number of layers. Due to the lack of significant entrainment, the overall filter efficiency for ten layers of the oleophobic filter in steady state is slightly higher than efficiency for ten layers of the oleophilic filter, even though the overall filter efficiency of the dry oleophobic filter was considerably lower. Excess differential pressure increased slightly with number of layers, due to an increased  $\Delta p_{\text{channel}}$ ,  $\Delta p_{\text{jump}}$  is independent of the number of layers. When reaching steady state differential pressure decreases slightly. This effect might be due to a redistribution of oil inside the filter and needs further investigation.

#### 4. Summary and conclusions

Experimental studies were carried out to determine the evolution of overall droplet penetration of oil mist filters with different media properties with regard to the oil transport mechanisms and its dependence on the operating conditions of the filters. The experiments were performed using two types of glass fiber filter media, one oleophilic and one oleophobic. Investigated parameters were filter face velocity and oil loading rate, with velocities ranging from 10 to 40 cm/s and oil loading rates between 60 and 195 mg/(m<sup>2</sup>s). Furthermore, media thickness was varied by varying the number of filter layers between 4 and 10 layers of filter material. The results show that oil transport mechanisms directly affect filter penetration and that the findings on the effects of operating conditions and media properties of oil mist filters on pressure drop concluded by Kampa et al. [1] and Kolb et al. [4] can be transferred to filter overall separation efficiency. The effects of the formation of oil channels and an oil film on differential pressure and overall penetration have been observed for both oleophilic and oleophobic filters. In the stage of operation when channels are formed, overall penetration increases. The deposition and coalescence of droplets and the subsequent transport of oil through the filter media in channel like structures leads to a loss of collector surface and an increase of internal velocities inside the media. The formation of a liquid film however improves deposition through impaction of droplets on the film. It was found that operating conditions affect the evolution of overall filter penetration through the deposition and transport of oil inside the filter media. Increasing velocities lead to decreasing saturations in steady state and thus less deterioration of overall filter efficiency in the channel stage. When transitioning to steady state, the MPPS of the filters shifts to smaller sizes. The difference between dry state MPPS and steady state MPPS and the difference in efficiency at the MPPS in dry and steady state decrease with increasing velocities, and higher efficiencies are reached for sizes bigger than the MPPS when transitioning to steady state. The effect of loading rate was not as significant as the effect of velocity, the increase of overall penetration in the channel stage however was slightly higher at higher loading rates for both types of media. When increasing the thickness of the filter by adding more layers of filter material, the length of oil channels is

increased, which results in a stronger increase of penetration in the channel stage for both types of media. For a high number of oleophilic filter layers and thus, high overall efficiencies it has been shown that secondary penetration due to entrainment of droplets by bursting bubbles is considerably higher than primary penetration of droplets through the filter, while no significant entrainment was measured for oleophobic filters.

#### References

- [1] D. Kampa, S. Wurster, J. Buzengeiger, J. Meyer, G. Kasper, Pressure drop and liquid transport through coalescence filter media used for oil mist filtration, *Int. J. Multiph. Flow* 58 (2014) 313–324.
- [2] C.R. Mackerer, Health effects of oil mists: a brief review, *Toxicol. Ind. Health* 5 (3) (1989) 429–440.
- [3] N. Kazerouni, T.L. Thomas, S.A. Petralia, R.B. Hayes, Mortality among workers exposed to cutting oil mist: update of previous reports, *Am. J. Ind. Med.* 38 (2000) 410–416.
- [4] H.E. Kolb, J. Meyer, G. Kasper, Flow velocity dependence of the pressure drop of oil mist filters, *Chem. Eng. Sci.* 166 (2017) 107–114.
- [5] H. Mohrmann, Beladung von Faserfiltern mit Aerosolen aus flüssigen Partikeln, *Staub Reinh. der Luft* 30 (1970) 317–321.
- [6] R. Gougeon, D. Boulaud, A. Renoux, Theoretical and experimental study of fibrous filters loading with liquid aerosols in the inertial regime, *J. Aerosol Sci.* 25 (Suppl. 1) (1994) 189–190.
- [7] P. Contal, J. Simao, D. Thomas, T. Frising, S. Callé, J.C. Appert-Collin, D. Bémer, Clogging of fibre filters by submicron droplets. Phenomena and influence of operating conditions, *J. Aerosol Sci.* 35 (2004) 263–278.
- [8] M. Boundy, D. Leith, D. Hands, M. Gressel, G.E. Burroughs, Performance of industrial mist collectors over time, *Appl. Occup. Environ. Hyg.* 15 (12) (2010) 928–935.
- [9] T. Frising, D. Thomas, D. Bémer, P. Contal, Clogging of fibrous filters by liquid aerosol particles: experimental and phenomenological modelling study, *Chem. Eng. Sci.* 60 (2005) 2751–2762.
- [10] S. Wurster, J. Meyer, H.E. Kolb, G. Kasper, Bubbling vs. blow-off – on the relevant mechanism(s) of drop entrainment from oil mist filter media, *Sep. Purif. Technol.* 152 (2015) 70–79.
- [11] S. Wurster, J. Meyer, G. Kasper, On the relationship of drop entrainment with bubble formation rates in oil mist filters, *Sep. Purif. Technol.* 179 (2017) 542–549.
- [12] J.R. Conder, T.P. Liew, Fine mist filtration by wet filters. II. Efficiency of fibrous filters, *J. Aerosol Sci.* 20 (1989) 45–57.
- [13] A. Charvet, Y. Gonthier, A. Bernis, E. Gonze, Filtration of liquid aerosols with a horizontal fibrous filter, *Chem. Eng. Res. Des.* 86 (2008) 569–576.
- [14] A. Charvet, Y. Gonthier, E. Gonze, A. Bernis, Experimental and modelled efficiencies during the filtration of a liquid aerosol with a fibrous media, *Chem. Eng. Sci.* 65 (2010) 1875–1886.

## Repository KITopen

Dies ist ein Postprint/begutachtetes Manuskript.

Empfohlene Zitierung:

Penner, T.; Meyer, J.; Kasper, G.; Dittler, A.  
[Impact of operating conditions on the evolution of droplet penetration in oil mist filters.](#)  
2019. Separation and purification technology, 211.  
[doi: 10.5445/IR/1000087594](https://doi.org/10.5445/IR/1000087594)

Zitierung der Originalveröffentlichung:

Penner, T.; Meyer, J.; Kasper, G.; Dittler, A.  
[Impact of operating conditions on the evolution of droplet penetration in oil mist filters.](#)  
2019. Separation and purification technology, 211, 697–703.  
[doi: 10.1016/j.seppur.2018.10.037](https://doi.org/10.1016/j.seppur.2018.10.037)

Lizenzinformationen: [CC BY-NC-ND 4.0](#)